Joseph et al.

Supplementary Information

Figure S1. Timing of microtubule disassembly and abscission. HeLa cells stably expressing GFP-tubulin and GFP-CENP-A were synchronised with double thymidine block, transiently transfected with mCherry-MKLP1 and observed by time-lapse microscopy with 11 min (not shown) or 8 min (A and B) min intervals. Disassembly of midbody-associated microtubules outside the Flemming body was observed around 70 min after the midbody formation (64±24 and 82±20 (mean ± s.d., n =12) for the first and second disassembly, respectively). On the other hand, there was a large variation in the timing of abscission determined by the behaviour of the Flemming body (207 ± 131 min (mean ± s. d., n = 12) after the midbody formation; 4 cells: < 120 min, 4 cells: 120 to 240 min, 4 cells: 240 min to 480 min). In some cells, the Flemming body migrated away from the border between the daughter cells immediately after the disassembly of microtubules (**A**). In other cells, the Flemming body remained at the border showing back and forth movement between the two daughter cells for several hours before it migrated from the border to the more central cell cortex of one of the daughters (**B**). Green: tubulin and CENP-A. Red: MKLP1. Purple and blue dotted lines indicate the edges of the two daughter cells. Bar, 5 μm.

Figure S2. Timing of S710-monophosphorylation. (**A**) HeLa cells were released from metaphase arrest by MG132, fixed at the indicated time (min) after the average timing of the midbody formation that was determined by a separate time-lapse observation, and immunostained for S710-monophosphorylated MKLP1 (pS710) and tubulin. (**B**) The intensities of pS710 signal at the Flemming body and tubulin signal in the midbody microtubules were quantified by ImageJ. Mean and standard error were plotted (n > 90 for each time point).

Figure S3. (**A**) Schematic diagram of ARF6 internally tagged with mCherry. (**B, C**) Stills from time-lapse observation of HeLa cells that were co-transfected with GFP-Rab11a and mCherry-ARF6 (**B**) or with GFP-MKLP1 and mCherry-Rab11a (**C**). Colocalisation of Rab11a with ARF6 (**B**) or MKLP1 (**C**) was not detected at the Flemming bodies (arrow head and arrow). Bar, 10 μm.

Figure S4. (**A**) Yeast two-hybrid assays to test the interaction between MKLP1 fragments and ARF6. Growth on medium lacking histidine and supplemented with 3-aminotriazol (3AT) indicates an interaction between proteins fused to the activation domain (AD) and DNA-binding domain (DB). MKLP1-NT and CYK4-NT are human MKLP1 and CYK4/MgcRacGAP

fragments, respectively, as positive controls. (**B**) Yeast two-hybrid assays to test the effects of the MKLP1 mutations in the ARF6-binding domain on the interaction with ARF6.

Figure S5. Co-immunoprecipitation between HsCYK-4/MgcRacGAP and the MKLP1 mutants. HeLa cells were transfected with plasmids encoding GFP or GFP-MKLP1s (wild type (WT), V786A or S710A&V786A mutants) and synchronised at M-phase by a thymidine block and release followed by nocodazole arrest. GFP or GFP-MKLP1s were immunoprecipitated by GFP-Trap beads . Samples were analysed by western-blotting with anti-GFP (JL-8, Clontech) and anti-HsCYK-4/MgcRacGAP (Mishima et al., 2002) antibodies. M: marker for electrophoresis.

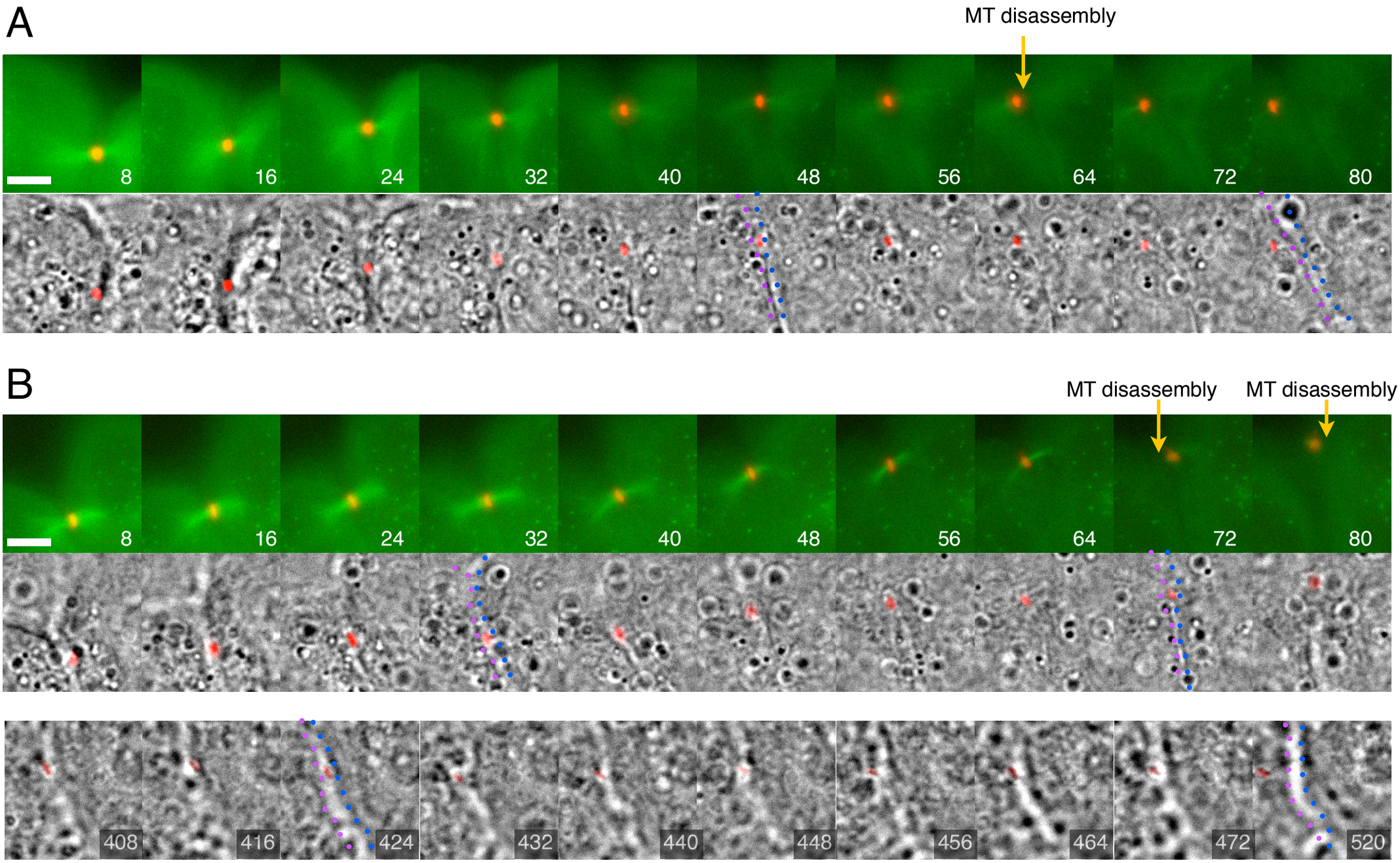

Joseph et al. Figure S1

A

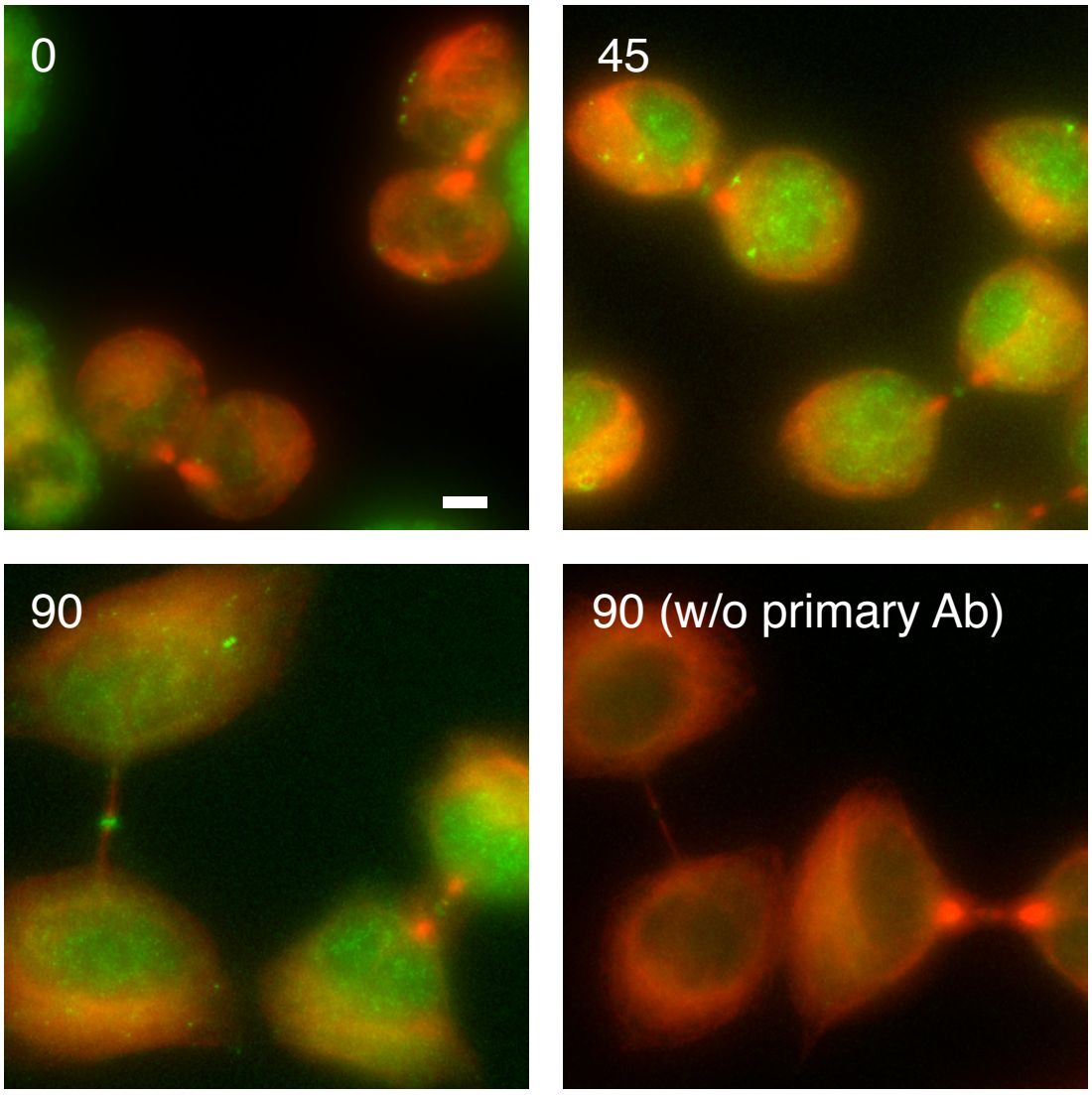

B

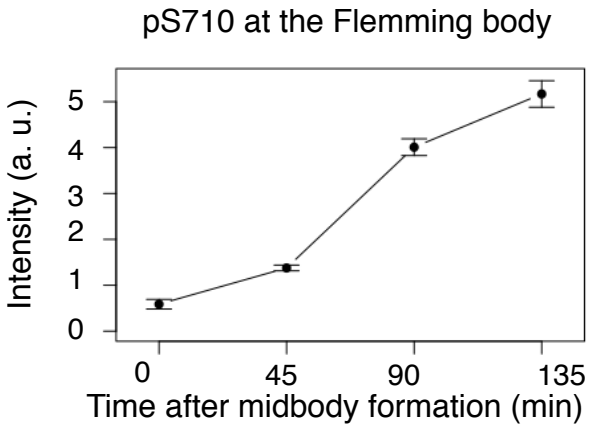

C

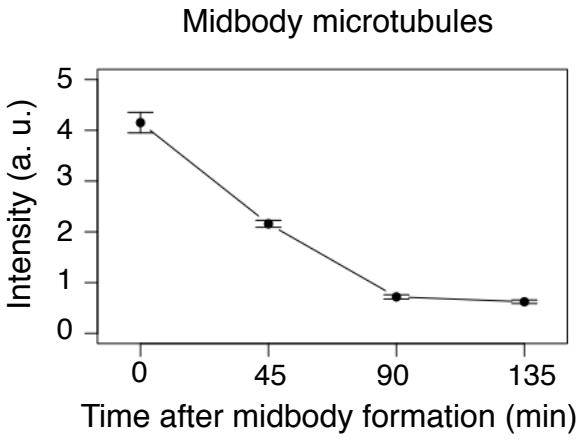

Joseph et al. Figure S2

A

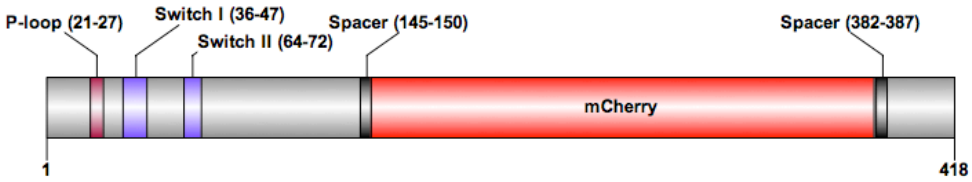

B

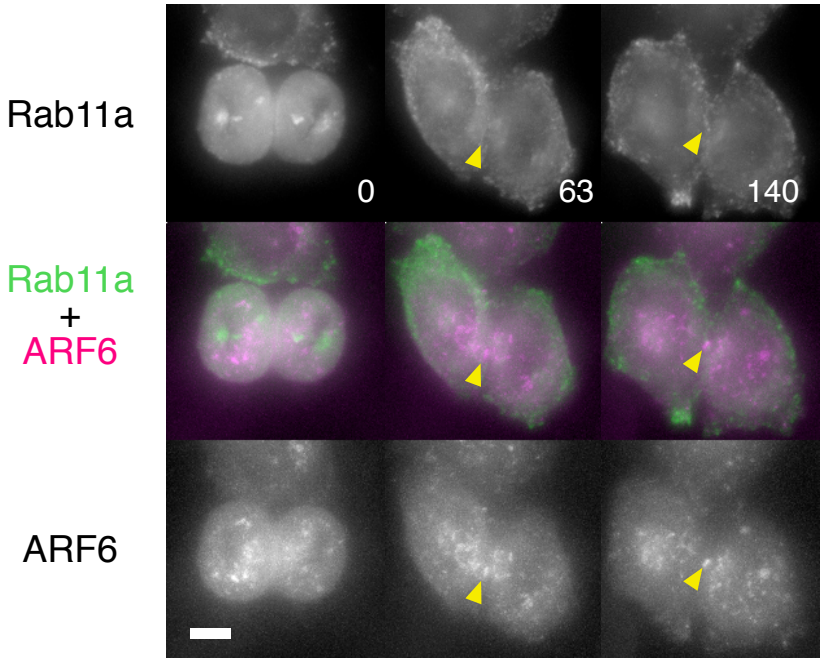

C

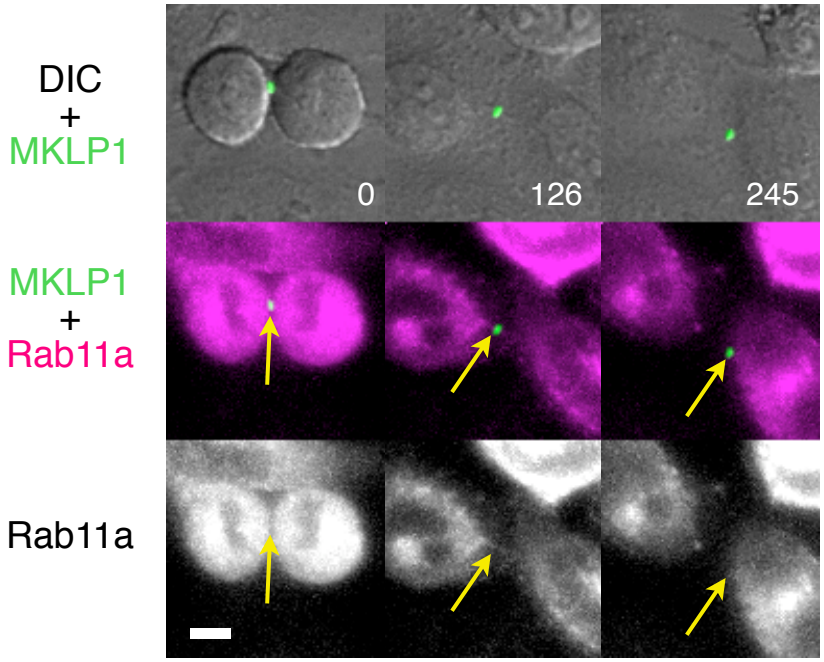

Joseph et al. Figure S3

A

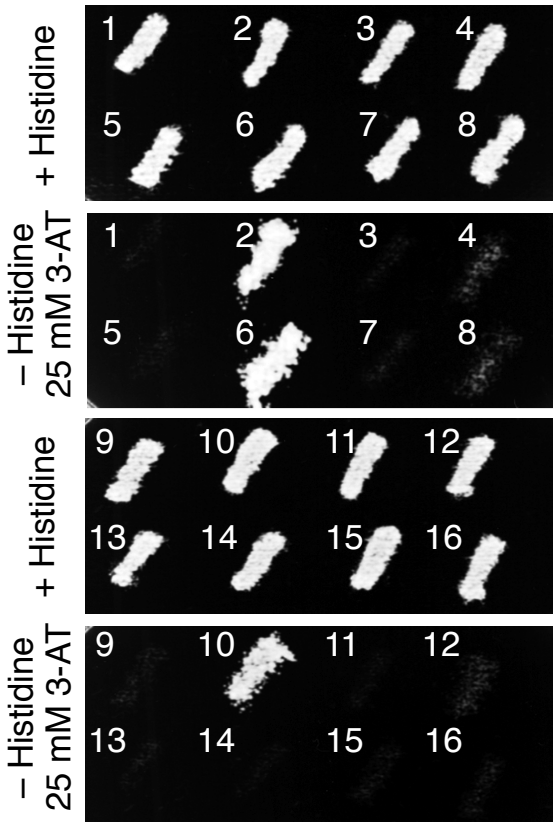

	AD		DB
1	MKLP1-CF2	x	ARF6-T27N
2	MKLP1-CF2	x	ARF6-Q67L
3	MKLP1-CF3	x	ARF6-T27N
4	MKLP1-CF3	x	ARF6-Q67L
5	MKLP1-CF9	x	ARF6-T27N
6	MKLP1-CF9	x	ARF6-Q67L
7	MKLP1-CF15	x	ARF6-T27N
8	MKLP1-CF15	x	ARF6-Q67L

	AD		DB
9	empty	x	ARF6-T27N
10	MKLP1-NT	x	CYK4-NT
11	empty	x	ARF6-T27N
12	empty	x	ARF6-Q67L
13	MKLP1-CF2	x	empty
14	MKLP1-CF3	x	empty
15	MKLP1-CF9	x	empty
16	MKLP1-CF15	x	empty

B

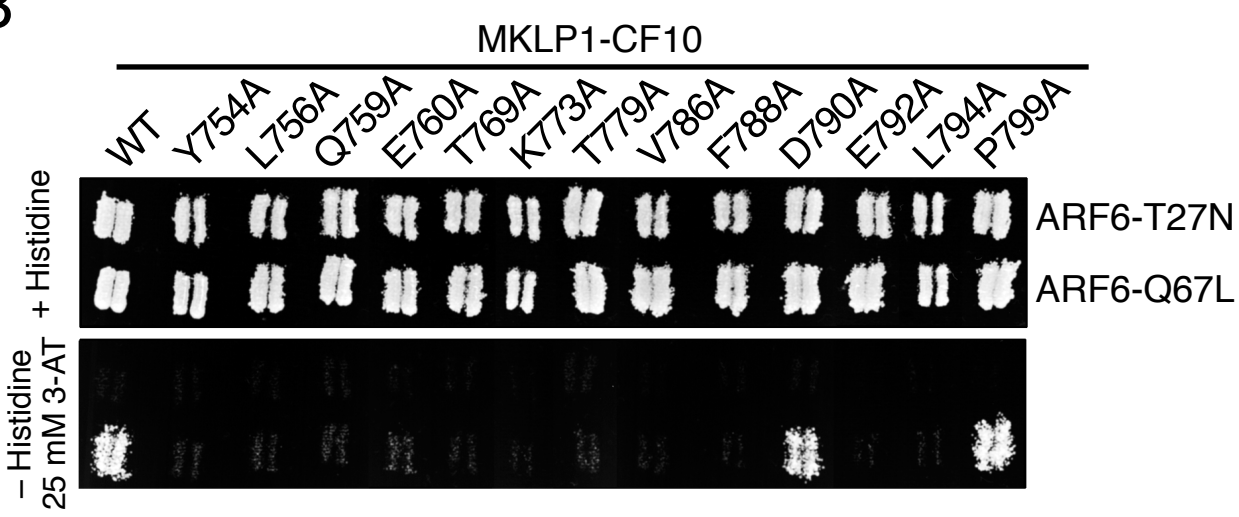

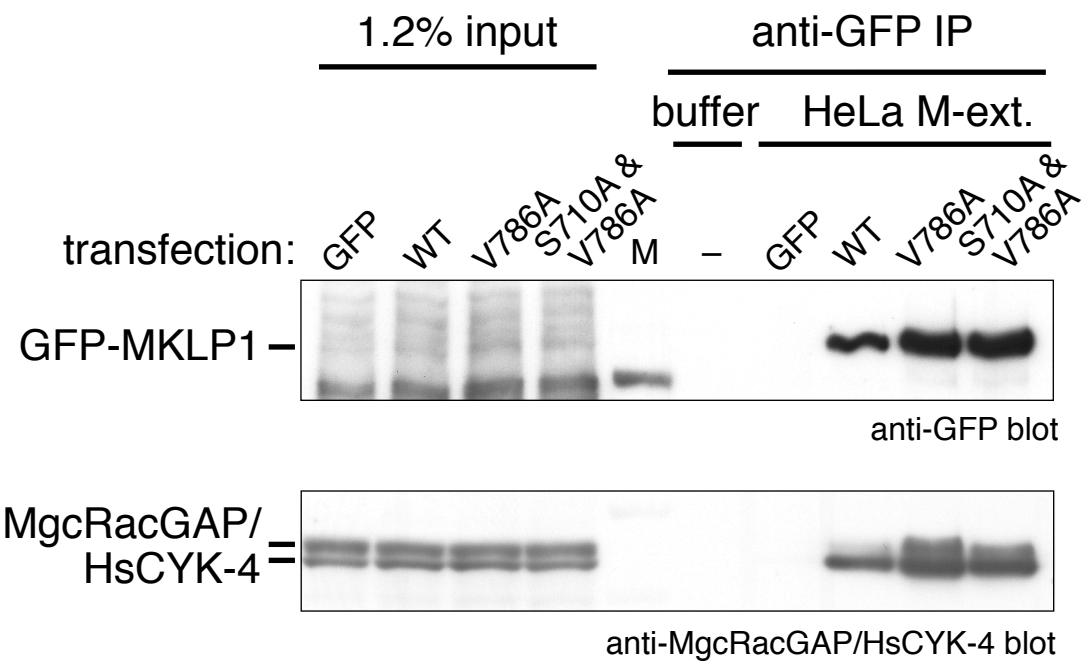

Joseph et al. Figure S5